

BCS pairing state in an asymmetric binary Bose gas

Zesheng Shen(沈泽盛) and Lan Yin(尹澜)

Citation: Chin. Phys. B, 2026, 35 (**4**): 046701. DOI: 10.1088/1674-1056/ae0160
http://cpb.iphy.ac.cn; http://iopscience.iop.org/cpb

What follows is a list of articles you may be interested in

Pairing transitions in a binary Bose gas

Zesheng Shen(沈泽盛) and Lan Yin(尹澜)
Chin. Phys. B, 2025, 34 (**10**): 106702. DOI: 10.1088/1674-1056/ade075

Three-dimensional ResNet for efficient prediction of ground state phases in multicomponent dipolar spinor BECs

Chengji Liao(廖承继), Tiantian Li(李甜甜), Xiao-Dong Bai(柏小东), and Yunbo Zhang(张云波)
Chin. Phys. B, 2025, 34 (**7**): 076701. DOI: 10.1088/1674-1056/adc7f9

Spinor *F*=1 Bose-Einstein condensates loaded in two types of radially-periodic potentials with spin-orbit coupling

Ji-Guo Wang(王继国), Yue-Qing Li(李月晴), Han-Zhao Tang(唐翰昭), and Ya-Fei Song(宋亚飞)
Chin. Phys. B, 2021, 30 (**10**): 106701. DOI: 10.1088/1674-1056/ac1411

Bose-Einstein condensates under a non-Hermitian spin-orbit coupling

Hao-Wei Li(李浩伟) and Jia-Zheng Sun(孙佳政)
Chin. Phys. B, 2021, 30 (**6**): 066702. DOI: 10.1088/1674-1056/abd7e4

Propagation of dark soliton interacting with domain wall in two immiscible Bose-Einstein condensates

Lang Zheng(郑浪), Yi-Cai Zhang(张义财), Chao-Fei Liu(刘超飞)
Chin. Phys. B, 2019, 28 (**11**): 116701. DOI: 10.1088/1674-1056/ab457e

---

BCS pairing state in an asymmetric binary Bose gas

Zesheng Shen(沈泽盛) and Lan Yin(尹澜)†

School of Physics, Peking University, Beijing 100871, *China*

(Received 16 May 2025; revised manuscript received 26 August 2025; accepted manuscript online 2 September 2025)

The BCS pairing state has been predicted to be stable in a symmetric binary Bose gas with the intraspecies repulsion and interspecies attraction. In experiments, the binary Bose gases are generally asymmetric. In this work, we study the pairing state in a dilute asymmetric binary Bose system with the intraspecies repulsions and interspecies attraction and show that it is stable in a certain region of the phase space. We find that there always exists a best density ratio for given total density and coupling constants, where the temperature width of the BCS region is maximized. At the best density ratio, both components have the almost same ideal BEC temperature. We also found that there are two critical density ratios where the BCS phase vanishes. The stability of the BCS state against pairing fluctuations is shown by expanding the Helmholtz free energy of BCS state near the normal state and proving that it is a local minimum point.

Keywords: pairing states, Bose–Einstein condensates

PACS: 67.85.–d, 03.75.Hh

DOI: 10.1088/1674-1056/ae0160 **CSTR:** 32038.14.CPB.ae0160

1. Introduction

Conventional superconductivity was successfully explained by the BCS (Bardeen–Cooper–Schrieffer) pairing theory in 1957.[1] Since then, the pairing states in various superconductors and fermionic superfluids have been intensively studied. After the successful experimental realization of BEC (Bose–Einstein condensation) in the ^{23}Na and ^{87}Rb system in 1995,[2,3] ultracold atoms have provided an ideal platform to explore novel quantum states including the pairing state. By the Feshbach resonance technique in ultracold atoms,[4–6] the interaction between atoms can be tuned by the external magnetic field. The BEC–BCS crossover[7–9] in Fermi gases has been successfully achieved in experiment, and the molecular BEC state was observed.[10–12] Theoretical studies were also carried out on the BCS[13–16] and molecular BEC[17–21] states of Bose system. In a single-component homogeneous Bose gas,[14,19,20] the molecular BEC state was found stable with the repulsive interaction. However, the BCS pairing state with the attractive interaction was found unstable due to negative compressibility. In experiments, the heavy three-body loss occurs near the resonance, making it hard to detect these states in Bose gases.

Binary Bose systems have provided a platform to study quantum droplets.[22,23] In a binary quantum droplet, the mean-field energy is negative, but the Lee–Huang–Yang energy is repulsive and making it stable.[24,25] The stability of phonon excitation is restored due to a higher-order effect.[26–30] In our previous work,[16] we predicted that the stable BCS state could exist in a symmetric binary Bose system, where the intra-species repulsion overcomes the inter-species attraction making the system mechanically stable. In current experiments, the binary Bose gases have asymmetric intraspecies interactions. In this work, we study an asymmetric binary Bose system in which the mass, density and intraspecies coupling constants can be all different for the two components. In the mean-field approximation, we find that for the fixed total density and coupling constants, there always exists a best density ratio of the two components, at which the temperature width of the BCS region is at maximum, close to where both components share the same ideal BEC temperature. Furthermore, we show that the BCS state vanishes at two critical density ratios. By expansion of the Helmholtz free energy, we find that the BCS state is always stable compared to the normal state. The experimental implications are discussed near the end.

2. Mean-field calculation of BCS state

2.1. General Hamiltonian

We consider a dilute asymmetric binary Bose gas. In the grand canonical ensemble, the single-particle Hamiltonian is given by

$$H_0 = \sum_{\boldsymbol{k},i} (\varepsilon_{i\boldsymbol{k}} - \mu_i)\, c^\dagger_{i\boldsymbol{k}} c_{i\boldsymbol{k}}, \tag{1}$$

where $\varepsilon_{i\boldsymbol{k}} = \hbar^2\boldsymbol{k}^2/2m_i$ represents the kinetic energy of the i-th component, $c_{i\boldsymbol{k}}$ is the Bose annihilation operator of the i-th component, and μ_i is the chemical potential of the i-th component.

Under the s-wave approximation, the intra- and inter-species interactions are contact potential potentials given by

$$H_{\text{intra}} = \sum_{i,\boldsymbol{k}_1\boldsymbol{k}_2\boldsymbol{k}_3} \frac{g_{ii}}{2V} c^\dagger_{i\boldsymbol{k}_1} c^\dagger_{i\boldsymbol{k}_2} c_{i\boldsymbol{k}_3} c_{i\boldsymbol{k}_1+\boldsymbol{k}_2-\boldsymbol{k}_3}, \tag{2}$$

†Corresponding author. E-mail: yinlan@pku.edu.cn

© 2026 Chinese Physical Society and IOP Publishing Ltd. All rights, including for text and data mining, AI training, and similar technologies, are reserved.

$$H_{\text{inter}} = \sum_{\boldsymbol{k}_1\boldsymbol{k}_2\boldsymbol{k}_3} \frac{g_{12}}{V} c^\dagger_{1\boldsymbol{k}_1} c^\dagger_{2\boldsymbol{k}_2} c_{2\boldsymbol{k}_3} c_{1\boldsymbol{k}_1+\boldsymbol{k}_2-\boldsymbol{k}_3}, \tag{3}$$

where $g_{ii} = 4\pi\hbar^2 a_{ii}/m_i$ and $g_{12} = 2\pi\hbar^2 a_{12}/m_\mu$ are the coupling constants of the system, V is the volume and m_μ is the reduced mass $m_\mu = m_1 m_2/(m_1+m_2)$. Here, different from the quantum droplets, we study in the mean-field stable region where the coupling constants satisfy $g_{11} > 0$, $g_{22} > 0$, $g_{12} < 0$, and $|g_{12}| < \sqrt{g_{11}g_{22}}$, ensuring a positive mean-field energy and compressibility.

2.2. Mean-field approximation

The inter-species attraction leads to pairing, the order parameter Δ in the BCS state is defined as

$$\Delta = \frac{g_{12}}{V}\sum_{\boldsymbol{k}} \langle c_{1\boldsymbol{k}} c_{2-\boldsymbol{k}}\rangle. \tag{4}$$

Without losing generality, we set Δ to be a negative real number, because it is always possible to make it real by a gauge transformation. In the mean-field approximation, the interaction terms are given by

$$H_{\text{intra}} = \sum_i \left(2g_{ii}n_i \sum_{\boldsymbol{k}} c^\dagger_{i\boldsymbol{k}} c_{i\boldsymbol{k}} - g_{ii} n_i^2 V\right), \tag{5}$$

$$\begin{aligned} H_{\text{inter}} = {} & \Delta \sum_{\boldsymbol{k}} \left(c^\dagger_{1\boldsymbol{k}} c^\dagger_{2-\boldsymbol{k}} + \text{h.c.}\right) - V\left(g_{12}n_1 n_2 + \frac{\Delta^2}{g_{12}}\right) \\ & + g_{12}\sum_{\boldsymbol{k}} \left(n_1 c^\dagger_{2\boldsymbol{k}} c_{2\boldsymbol{k}} + n_2 c^\dagger_{1\boldsymbol{k}} c_{1\boldsymbol{k}}\right), \end{aligned} \tag{6}$$

where n_i is the density of the i-th component. The mean-field Hamiltonian can be written as

$$H = \sum_{\boldsymbol{k}} B^\dagger_{\boldsymbol{k}} H_{\boldsymbol{k}} B_{\boldsymbol{k}} + E_{\text{B}}, \tag{7}$$

$$H_{\boldsymbol{k}} = \begin{pmatrix} \varepsilon_{1\boldsymbol{k}} - \mu_1' & \Delta \\ \Delta & \varepsilon_{2\boldsymbol{k}} - \mu_2' \end{pmatrix}, \tag{8}$$

where $B^\dagger_{\boldsymbol{k}} = \left(c^\dagger_{1\boldsymbol{k}}, c_{2-\boldsymbol{k}}\right)$, $\mu_i' = \mu_i - 2g_{ii}n_i + g_{12}n_{3-i}$ is the shifted chemical potential of the i-th component, and

$$\begin{aligned} E_{\text{B}} = {} & -\sum_{\boldsymbol{k}} \left(\varepsilon_{2\boldsymbol{k}} - \mu_2'\right) \\ & - V\left(\frac{\Delta^2}{g_{12}} + g_{11}n_1^2 + g_{22}n_2^2 + g_{12}n_1 n_2\right). \end{aligned}$$

The Hamiltonian Eq. (7) can be diagonalized by a general Bogoliubov transformation $\det\left(H_{\boldsymbol{k}} - E_{\boldsymbol{k}}\sigma_z\right) = 0$ and the quasi-particle excitation spectra are given by

$$\begin{aligned} E_{1,2\boldsymbol{k}} = {} & \pm\frac{\left(\varepsilon_{1\boldsymbol{k}} - \mu_1'\right) - \left(\varepsilon_{2\boldsymbol{k}} - \mu_2'\right)}{2} \\ & + \sqrt{\left[\frac{\left(\varepsilon_{1\boldsymbol{k}} - \mu_1'\right) + \left(\varepsilon_{2\boldsymbol{k}} - \mu_2'\right)}{2}\right]^2 - \Delta^2}, \end{aligned} \tag{9}$$

equations (7) and (9) are consistent with the symmetric case.[16] The order parameter satisfies $|\Delta| < \sqrt{\mu_1'\mu_2'}$, consistent with the symmetric case, $|\Delta| < |\mu'|$.[16] Nevertheless, the excitation spectra are no longer degenerated in the asymmetric system due to the difference in $\varepsilon_{i\boldsymbol{k}} - \mu_i'$.

The order parameter Δ and the particle densities can be determined from the following self-consistent equations:

$$n_1 = \frac{1}{2V}\sum_{\boldsymbol{k}} \left[\left(\frac{\eta_{\boldsymbol{k}}}{A_{\boldsymbol{k}}} + 1\right) f_{1\boldsymbol{k}} + \left(\frac{\eta_{\boldsymbol{k}}}{A_{\boldsymbol{k}}} - 1\right)\left(f_{2\boldsymbol{k}} + 1\right)\right], \tag{10}$$

$$n_2 = \frac{1}{2V}\sum_{\boldsymbol{k}} \left[\left(\frac{\eta_{\boldsymbol{k}}}{A_{\boldsymbol{k}}} - 1\right)\left(f_{1\boldsymbol{k}} + 1\right) + \left(\frac{\eta_{\boldsymbol{k}}}{A_{\boldsymbol{k}}} + 1\right) f_{2\boldsymbol{k}}\right], \tag{11}$$

$$\frac{-m_\mu}{2\pi\hbar^2 a_{12}} = \frac{1}{V}\sum_{\boldsymbol{k}} \left[\frac{1}{2A_{\boldsymbol{k}}}\left(f_{1\boldsymbol{k}} + f_{2\boldsymbol{k}} + 1\right) - \frac{1}{2\varepsilon_{\boldsymbol{k}}}\right], \tag{12}$$

where $\eta_{i\boldsymbol{k}} = \varepsilon_{i\boldsymbol{k}} - \mu_i'$, $\eta_{\boldsymbol{k}} = (\eta_{1\boldsymbol{k}} + \eta_{2\boldsymbol{k}})/2$, $A_{\boldsymbol{k}} = \sqrt{\eta_{\boldsymbol{k}}^2 - \Delta^2}$, $\varepsilon_{\boldsymbol{k}} = \hbar^2\boldsymbol{k}^2/4m_\mu$, and $f_{i\boldsymbol{k}} = 1/(\mathrm{e}^{\beta E_{i\boldsymbol{k}}} - 1)$ stands for the Bose distribution of quasi-particles on the i-th branch where $\beta = 1/k_{\text{B}}T$. In Eq. (12), we have included the renormalization relationship of the coupling constant

$$\frac{1}{g_{12}} = \frac{m_\mu}{2\pi\hbar^2 a_{12}} - \frac{1}{2V}\sum_{\boldsymbol{k}} \frac{1}{\varepsilon_{\boldsymbol{k}}}.$$

As we have pointed out,[16] the BCS state exists between two critical temperatures in the symmetric case. The BCS-normal phase transition takes place at the upper critical temperature where $\Delta = 0$ and $E_{i\boldsymbol{k}} = \varepsilon_{i\boldsymbol{k}} - \mu_i'$. At the lower critical temperature, the energy gap in the excitation spectrum vanishes $E_{i0} = 0$ and the system turns into a mixture of atom condensate and BCS pairs. In the asymmetric system, the BCS phase only exists in certain region of the T–n_1/n_2 plane for the fixed total density $n = n_1 + n_2$ as discussed in the next section. In general, the two excitation branches are both gapped in the BCS region, which means $E_{i\boldsymbol{k}=0} > 0$. The upper boundary of the BCS phase locates at $\Delta = 0$ where the normal-BCS phase transition takes place. The lower boundary of the BCS phase is reached when one excitation branch is gapless, $E_{i\boldsymbol{k}=0} = 0$, where there is no energy cost to turn atoms into the condensate, and the order parameter satisfies the condition $\Delta = -\sqrt{\mu_1'\mu_2'}$.

2.3. Numerical results

So far binary quantum droplets have been realized in two systems, ^{39}K–^{39}K and ^{23}Na–^{87}Rb mixtures. We study the BCS states in both dilute systems with experimentally feasible parameters. In the symmetric case, the BCS phase exists above the ideal BEC temperature. Here we first numerically determine the boundaries of the BCS phases in these two systems for the fixed total density and coupling constants. As shown in Fig. 1(a), in the binary ^{39}K gas, the normal-BCS transition temperature is at maximum when the two components have the same density, $n_1/n_2 = 1$, where $n = n_1 + n_2$ and

$$T_{\text{B}n} = \frac{2^{-2/3}\pi\hbar^2}{m_\mu k_{\text{B}}}\left(\frac{n}{\zeta(3/2)}\right)^{2/3}.$$

The lower boundary of the BCS state is rather flat. In contrast, for the ^{23}Na–^{87}Rb mixture, the normal-BCS transition temperature is a monotonous function of n_1/n_2 as shown in Fig. 1(b). In both cases, the temperature width of the BCS phase has a maximum as a function of the density ratio n_1/n_2 for the fixed total density and interactions, as shown in Figs. 2(a) and 2(b) where $\left|na_{12}^3\right| = -1.20\times10^{-5}$. This best density ratio is close to $n_2/n_1 = \left(m_2/m_1\right)^{3/2}$. For a single component Bose gas, the ideal BEC-transition temperature is given by $T_{\rm B} = 2\pi\hbar^2 n^{2/3}/mk_{\rm B}\zeta^{2/3}(3/2)$, where n is the density of particle numbers. Therefore, the best density ratio corresponds to the ratio where the two components share the same ideal BEC temperature.

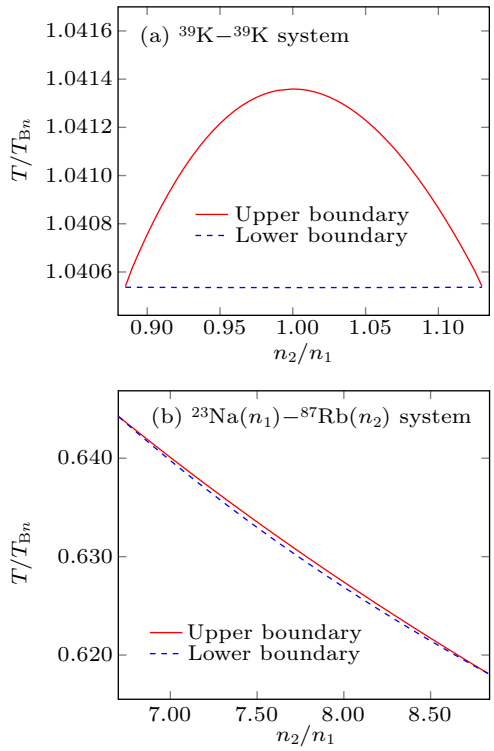


Fig. 1. The normal-BCS transition temperate (upper boundary) and BCS-mixture transition temperature (lower boundary) *versus* the ratio of particle number density n_2/n_1 in ^{39}K–^{39}K and ^{23}Na–^{87}Rb systems, numerically calculated at $\left|na_{12}^3\right| = -1.20\times10^{-5}$, for the fixed total density n and coupling constants.

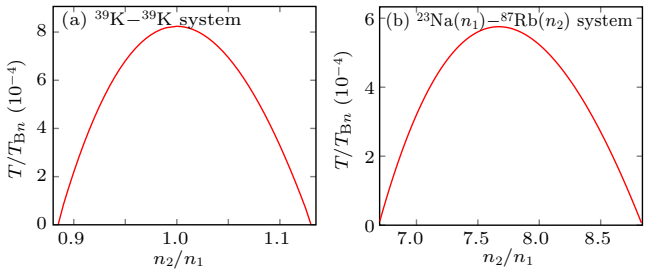


Fig. 2. The width of BCS region $\Delta T/T_{Bn}$ *versus* the ratio of particle number density n_2/n_1 in ^{39}K–^{39}K and ^{23}Na–^{87}Rb systems, numerically calculated at $\left|na_{12}^3\right| = -1.20\times10^{-5}$, for the fixed total density n and coupling constants.

At two critical density ratios, the upper and lower boundaries of the BCS phase overlap and terminate, which corresponds to the condition $\sqrt{\mu_1'\mu_2'} = 0$, with $\mu_1' = \Delta = 0$ at one side and $\mu_2' = \Delta = 0$ at the other side. At the critical point $\mu_2' = 0$, equations (10) and (11) recover the equation for the normal state,

$$n_i = \left(\frac{m_i}{2\beta\pi^{1/3}\hbar^2}\right)^{3/2} {\rm Li}_{3/2}\left(e^{\beta\mu_i'}\right), \tag{13}$$

where ${\rm Li}_{3/2}(x)$ is the polylogarithmic function defined by ${\rm Li}_s(z) = \sum_{k=1}^{\infty} z^k/k^s$. The right-hand side of Eq. (12) is approximately given by

$$\frac{-m_\mu}{2\pi\hbar^2 a_{12}} = \frac{8m_1m_2}{8\beta\hbar^4}\sqrt{\frac{\hbar^2}{-2m_1\mu_1'}}. \tag{14}$$

Therefore, the density ratio of this critical point is given by

$$\frac{n_2}{n_1} = \left(\frac{m_2}{m_1}\right)^{3/2}\frac{{\rm Li}_{3/2}\left(e^{\beta\mu_1'}\right)}{{\rm Li}_{3/2}(1)}, \tag{15}$$

where

$$\beta\mu_1' = -\frac{4\pi^{1/3}(m_1+m_2)^2\left(n_2a_{12}^3\right)^{2/3}}{m_1m_2{\rm Li}_{3/2}^{2/3}(1)}. \tag{16}$$

In the dilute region, equations (15) and (16) can be expanded in terms of the gas parameter na_{12}^3, and this critical density ratio is approximately given by

$$\frac{n_2}{n_1} \approx \left(\frac{m_2}{m_1}\right)^{3/2}\left[1-\frac{2.714\pi^{1/6}(m_1+m_2)\left(na_{12}^3\right)^{1/3}}{m_2^{1/2}\left(m_2^{3/2}+m_2^{3/2}\right)^{2/3}{\rm Li}_{3/2}^{2/3}(1)}\right]. \tag{17}$$

In the same way, the other critical density ratio can be obtained analytically,

$$\frac{n_2}{n_1} = \left(\frac{m_2}{m_1}\right)^{3/2}\left[1+\frac{2.714\pi^{1/6}(m_1+m_2)\left(na_{12}^3\right)^{1/3}}{m_1^{1/2}\left(m_1^{3/2}+m_2^{3/2}\right)^{2/3}{\rm Li}_{3/2}^{2/3}(1)}\right]. \tag{18}$$

In Fig. 1(a), these critical density ratios are $n_2/n_1 = 0.890$ and $n_2/n_1 = 1.110$, consistent with the expansion results $n_2/n_1 = 0.913$ and $n_2/n_1 = 1.087$ from Eqs. (17) and (18). Similarly, the numerical boundaries in Fig. 1(b) are $n_2/n_1 = 6.702$ and $n_2/n_1 = 8.832$, close to the analytical results from Eq. (17) and Eq. (18) $n_2/n_1 = 6.990$ and $n_2/n_1 = 8.444$.

In the dilute limit $na_{12}^3 \to 0$, as shown from Eqs. (17) and (18), the BCS region shrinks towards the point $n_2/n_1 = \left(m_2/m_1\right)^{3/2}$, where the two components share the same ideal BEC temperature. Therefore, the best density ratio lies near the density ratio $n_2/n_1 = \left(m_2/m_1\right)^{3/2}$. In Fig. 2(a), this best density ratio is $n_2/n_1 = \left(m_2/m_1\right)^{3/2} = 1$; in Fig. 2(b), it is $n_2/n_1 = 7.672$, near the point $n_2/n_1 = \left(m_2/m_1\right)^{3/2} = 7.357$. This condition could be helpful for searching the BCS region in experimental and numerical setups. Furthermore, we numerically calculate the best density ratio n_2/n_1 and the corresponding width of the BCS region $\Delta T/T_{Bn}$ as functions of the interspecies coupling constant. As shown in Figs. 3(a) and (3(b)), the temperature width of the BCS region increase significantly as the interaction strength increases. In contrast, in

Figs. 1(a) and 1(b), the interspecies interaction is rather weak, $1/(n/2)^{1/3}a_{12} = -55$, and the temperature width of the BCS region is small. The BCS region of the system would be more easily detected in experiments with strong interactions, but in practice near the resonance the three-body loss is severe.

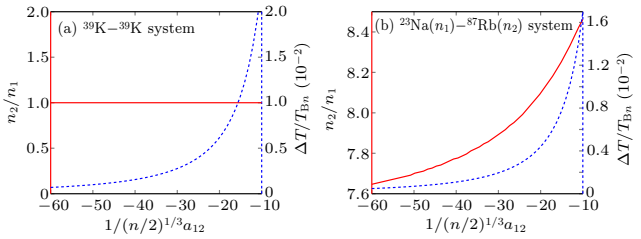


Fig. 3. The best density ratio n_2/n_1 and width of BCS region $T/T_{\mathrm{B}n}$ *versus* the gas parameter $\left(na_{12}^3/2\right)^{-1/3}$ in ^{39}K–^{39}K and ^{23}Na–^{87}Rb systems. The red solid line represents the density ratio n_2/n_1 leading to max width of BCS region and is a constantly $n_2/n_1 = 1$ in Fig. 3(a). The blue dashed line marks the max width of BCS region calculated under the best density ratio. The width significantly increases with the coupling constant.

3. Stability of BCS state

To study stability of the BCS state against the normal state at temperature above the BEC temperature, we follow Landau's theory of phase transition to show its free energy is a local minimum point compared to the normal state. We consider the Helmholtz free energy in the canonical ensemble $\langle F\rangle = \langle H - TS\rangle$ where the densities n_1 and n_2 are fixed. The free energy of the BCS state is given by

$$\begin{aligned} F &= \sum_{i\boldsymbol{k}} E_{\boldsymbol{k}i} f_{i\boldsymbol{k}} + \sum_{\boldsymbol{k}} (E_{2\boldsymbol{k}} - \eta_{2\boldsymbol{k}}) \\ &\quad - k_{\mathrm{B}}T \sum_{\boldsymbol{k},i} \left[(f_{i\boldsymbol{k}}+1)\ln(f_{i\boldsymbol{k}}+1) - f_{i\boldsymbol{k}}\ln(f_{i\boldsymbol{k}})\right] \\ &\quad + \sum_i \mu_i N_i - V\left(\frac{\Delta^2}{g_{12}} + g_{11}n_1^2 + g_{22}n_2^2 + g_{12}n_1n_2\right), \end{aligned} \tag{19}$$

where $\eta_{i\boldsymbol{k}} = \varepsilon_{i\boldsymbol{k}} - \mu_i'$ and $\eta_{\boldsymbol{k}} = (\eta_{1\boldsymbol{k}} + \eta_{2\boldsymbol{k}})/2$. To compare the free energy between BCS state and normal state, we denote $\delta\mu_i = \mu_i - \mu_{i0}$, where 0 represents the quantity taken in the normal state. We expand the free energy up to the forth order of the pairing order parameter Δ near the normal state. Therefore, the expanded energy spectrum is

$$\delta E_{i\boldsymbol{k}} = \delta\eta_{i\boldsymbol{k}} - \frac{\Delta^2}{2\eta_{i\boldsymbol{k}0}} + \frac{\delta\eta_{i\boldsymbol{k}}\Delta^2}{2\eta_{i\boldsymbol{k}0}^2} - \frac{\Delta^4}{8\eta_{i\boldsymbol{k}0}^3}$$

and $\delta\eta_{i\boldsymbol{k}} = -\delta\mu_i$. Any term of the order higher than the quadratic order of $\delta\mu_i$ is omitted and we will show $\delta\mu_i \sim \Delta^2$ in the latter. After the substitution, the expansion of the Helmholtz free energy is given by

$$\begin{aligned} \delta F &= \Delta^2\left[\frac{-V}{g_{12}} + \frac{1}{2}\sum_{\boldsymbol{k},i}\coth\left(\frac{\beta\eta_{i\boldsymbol{k}0}}{2}\right)\right. \\ &\quad \left.\times\left(\frac{-1}{2\eta_{i\boldsymbol{k}0}} + \frac{\delta\eta_{\boldsymbol{k}}}{2\eta_{i\boldsymbol{k}0}^2} - \frac{\Delta^2}{8\eta_{i\boldsymbol{k}0}^3}\right)\right]. \end{aligned} \tag{20}$$

The relationship between $\delta\mu_i$ and Δ could be obtained by expanding Eqs. (10) and (11) because the densities are fixed in the canonical ensemble, leading to $\delta\mu_i = A_i\Delta^2$, where

$$A_i = \frac{\sum_{\boldsymbol{k}}\left[\frac{1}{2\eta_{\boldsymbol{k}0}^2}\left(\frac{f_{\boldsymbol{k}10}+f_{\boldsymbol{k}10}}{2}+\frac{1}{2}\right) - \frac{f_{\boldsymbol{k}i0}'}{2\eta_{\boldsymbol{k}0}}\right]}{\sum_{\boldsymbol{k}} f_{\boldsymbol{k}i0}'}, \tag{21}$$

and $f_{\boldsymbol{k}i0}' = -\beta f_{\boldsymbol{k}i0}^2 \mathrm{e}^{\beta\eta_{i\boldsymbol{k}0}}$.

After substituting $\delta\mu_i$ in Eq. (20), the expansion could be concisely expressed as

$$\delta F = \alpha'\Delta^2 + \beta'\Delta^4, \tag{22}$$

where

$$\begin{aligned} \alpha' &= -\left(\frac{V}{g_{12}} + \frac{1}{2}\sum_{\boldsymbol{k}i}\frac{\coth\left(\frac{\beta\eta_{i\boldsymbol{k}0}}{2}\right)}{2\eta_{\boldsymbol{k}0}}\right), \\ \beta' &= \sum_{\boldsymbol{k}i}\left(f_{i\boldsymbol{k}0}+\frac{1}{2}\right)\left(\frac{A_1+A_2}{4\eta_{\boldsymbol{k}0}^2} - \frac{1}{8\eta_{\boldsymbol{k}0}^3}\right). \end{aligned}$$

At the upper boundary where $\Delta = 0$, from Eq. (12), we have $\alpha' = 0$. As the shifted chemical potential of normal state μ_{i0}' decreases when the temperature decreases, the stability condition $\alpha' < 0$ is satisfied. The other stability condition of the BCS state is $\beta' > 0$. To show that it is also satisfied, we consider the dilute limit and take the approximation $f_{i\boldsymbol{k}0} \approx 1/\beta\eta_{i\boldsymbol{k}0}$ and $f_{\boldsymbol{k}i0}' \approx 1/\beta\eta_{i\boldsymbol{k}0}^2$. In this way, we obtain the expression for β',

$$\beta' \approx \frac{B(\gamma)\, m_\mu^4}{\beta\pi\hbar^8 k_0^5}, \tag{23}$$

where $\gamma = m_1/m_2$ and

$$\begin{aligned} B(\gamma) &= 2\left(f_2(\gamma) + f_2\left(\frac{1}{\gamma}\right)\right)\left(f_3(\gamma) + f_3\left(\frac{1}{\gamma}\right)\right) \\ &\quad - \frac{1}{2}f_4(\gamma)\, f_4\left(\frac{1}{\gamma}\right), \end{aligned} \tag{24}$$

$$k_0 = \sqrt{\frac{2m_1m_2}{\beta\hbar^2(m_1+m_2)}\sum_i \ln\frac{1}{8n_i}\left(\frac{2m_i}{\pi\beta\hbar^2}\right)^{3/2}}, \tag{25}$$

$$\begin{aligned} f_1(\gamma) &= \sqrt{\frac{1}{2(1+\gamma)^3}}, \\ f_2(\gamma) &= \frac{(1+\gamma)\left[f_1(\gamma) + f_1(1/\gamma)\right] + 1}{\left(1+\sqrt{(1+\gamma)/2}\right)^2}, \\ f_3(\gamma) &= \frac{1+\gamma}{\sqrt{(1+\gamma)/2}\left(1+\sqrt{(1+\gamma)/2}\right)^2}, \\ f_4(\gamma) &= \frac{(1+\gamma)\left(3+\sqrt{(1+\gamma)/2}\right)}{\left(1+\sqrt{(1+\gamma)/2}\right)^3}. \end{aligned} \tag{26, 27}$$

In the dilute limit, the coefficient β' is is proportional $B(\gamma)$ which is determined by the mass ratio γ. Equation (23) recovers the result $\beta' = \frac{V}{16\pi\beta\hbar^8 k_0^5}$ in the symmetric case.[16] As shown in Fig. 4, the function $B(\gamma)$ satisfies $B(\gamma) = B(\frac{1}{\gamma})$ and its minimum is given by $B(1) = 1$. Therefore , we prove that in the BCS state the stability condition $\beta' > 0$ holds in the dilute limit and the free energy is always located at a local minimum.

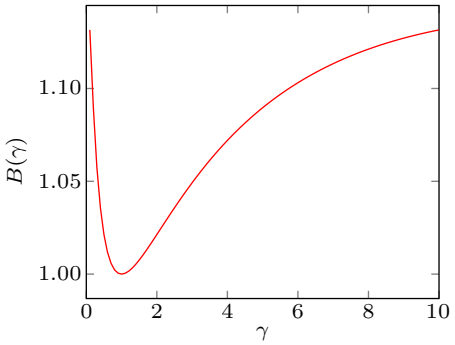


Fig. 4. The coefficient $B(\gamma)$ as a function of γ. The bottom point of the curve lies at $\gamma = 1$.

4. Discussion and conclusion

In experiment, the energy spectra of the binary Bose gas could be detected by modern energy-resolved tools on ultracold atoms such as RF spectroscopy[31] and Bragg spectroscopy.[32] The current difficulty in experiments is that the small gas parameter, $na^3 \sim 10^{-6}$, makes the temperature width of BCS region rather small, of the order of $10^{-3}T_{\mathrm{B}n}$. To make the state more detectable, the interactions need to be strengthened, but so far it is restricted by the three-body loss.[21] When temperature is below the lower boundary of the BCS phase, the system probably enters into a BCS–BEC mixture state as in the symmetric case,[16] which can be explored in future works.

In conclusion, we show that BCS state exists in a dilute asymmetric binary Bose gas with the intra-species repulsions and inter-species attraction. It is mechanically stable in the mean-field stable region when the inter-species attraction is weaker than the geometric means of the intra-species repulsions. We obtain the quasi-particle energy spectra of the asymmetric binary Bose system in the BCS state, which are generally non-degenerate, different from the symmetric system. Another difference is the phase diagram where the BCS phase only exists in certain region of the T–n_1/n_2 plane. For the coupling constants and total density, we show there exists a best density ratio where the temperature width of BCS region is maximized, near the ratio where two components share the same ideal BEC-transition temperature. The width of BCS region increases with the interspecies attraction. We find that at two critical density ratios the BCS phase vanishes. We obtain an approximate expression for the two critical density ratios, which converges to the best density ratio in the dilute limit. We also use Landau's phase-transition theory to investigate the stability of BCS phase and find it has lower free energy than the normal state.

References

[1] Bardeen J, Cooper L N and Schrieffer J R 1957 *Phys. Rev.* **108** 1175
[2] Anderson M H, Ensher J R, Matthews M R, Wieman C E and Cornell E A 1995 *Science* **269** 198
[3] Davis K B, Mewes M O, Andrews M R, van Druten N J, Durfee D S, Kurn D M and Ketterle W 1995 *Phys. Rev. Lett.* **75** 3969
[4] Pethick C J and Smith H 2008 *Bose-Einstein Condensation in Dilute Gases*, 2nd edn. (Cambridge University Press)
[5] O'Hara K M, Hemmer S L, Gehm M E, Granade S R and Thomas J E 2002 *Science* **298** 2179
[6] Bourdel T, Cubizolles J, Khaykovich L, Magalhães K M F, Kokkelmans S J J M F, Shlyapnikov G V and Salomon C 2003 *Phys. Rev. Lett.* **91** 020402
[7] Zwierlein M W, Abo-Shaeer J R, Schirotzek A, Schunck C H and Ketterle W 2005 *Nature* **435** 1047
[8] Regal C A, Greiner M and Jin D S 2004 *Phys. Rev. Lett.* **92** 040403
[9] Chin C, Bartenstein M, Altmeyer A, Riedl S, Jochim S, Denschlag J H and Grimm R 2004 *Science* **305** 1128
[10] Regal C A, Ticknor C, Bohn J L and Jin D S 2003 *Nature* **424** 47
[11] Strecker K E, Partridge G B and Hulet R G 2003 *Phys. Rev. Lett.* **91** 080406
[12] Cubizolles J, Bourdel T, Kokkelmans S J J M F, Shlyapnikov G V and Salomon C 2003 *Phys. Rev. Lett.* **91** 240401
[13] Evans W A B and Rashid R I M A 1973 *Journal of Low Temperature Physics* **11** 93
[14] Jeon G S, Yin L, Rhee S W and Thouless D J 2002 *Phys. Rev. A* **66** 011603
[15] Stoof H T C 1994 *Phys. Rev. A* **49** 3824
[16] Shen Z and Yin L 2025 *Chin. Phys. B* **34** 106702
[17] Radzihovsky L, Park J and Weichman P B 2004 *Phys. Rev. Lett.* **92** 160402
[18] Romans M W J, Duine R A, Sachdev S and Stoof H T C 2004 *Phys. Rev. Lett.* **93** 020405
[19] Yu Z Q and Yin L 2010 *Phys. Rev. A* **81** 023613
[20] Yin L 2008 *Phys. Rev. A* **77** 043630
[21] Xu K, Mukaiyama T, Abo-Shaeer J R, Chin J K, Miller D E and Ketterle W 2003 *Phys. Rev. Lett.* **91** 210402
[22] Semeghini G, Ferioli G, Masi L, Mazzinghi C, Wolswijk L, Minardi F, Modugno M, Modugno G, Inguscio M and Fattori M 2018 *Phys. Rev. Lett.* **120** 235301
[23] Guo Z, Jia F, Li L, Ma Y, Hutson J M, Cui X and Wang D 2021 *Phys. Rev. Res.* **3** 033247
[24] Petrov D S 2015 *Phys. Rev. Lett.* **115** 155302
[25] Petrov D S 2018 *Nat. Phys.* **14** 211
[26] Gu Q and Yin L 2020 *Phys. Rev. B* **102** 220503
[27] Xiong Y and Yin L 2022 *Phys. Rev. A* **105** 053305
[28] Zhang F and Yin L 2022 *Chin. Phys. Lett.* **39** 060301
[29] Zhang F and Yin L 2025 *Chin. Phys. Lett.* **42** 010302
[30] Zhang F and Yin L 2023 *Chin. Phys. Lett.* **40** 066701
[31] Shashi A, Grusdt F, Abanin D A and Demler E 2014 *Phys. Rev. A* **89** 053617
[32] Papp S B, Pino J M, Wild R J, Ronen S, Wieman C E, Jin D S and Cornell E A 2008 *Phys. Rev. Lett.* **101** 135301